

A common mechanism for CFTR potentiators

Han-I Yeh,¹ Yoshiro Sohma,^{1,2} Katja Conrath,³ and Tzyh-Chang Hwang¹

¹Dalton Cardiovascular Research Center and Department of Medical Pharmacology and Physiology, University of Missouri, Columbia, MO

²Department of Pharmaceutical Sciences, School of Pharmacy and Center for Medical Science, International University of Health and Welfare, Tochigi, Japan

³Galapagos NV, Mechelen, Belgium

Cystic fibrosis (CF) is a channelopathy caused by loss-of-function mutations of the cystic fibrosis transmembrane conductance regulator (CFTR) gene, which encodes a phosphorylation-activated and adenosine triphosphate (ATP)-gated chloride channel. In the past few years, high-throughput drug screening has successfully realized the first US Food and Drug Administration-approved therapy for CF, called ivacaftor (or VX-770). A more recent CFTR potentiator, GLPG1837 (*N*-(3-carbamoyl-5,5,7,7-tetramethyl-4,7-dihydro-5*H*-thieno[2,3-*c*]pyran-2-yl)-1*H*-pyrazole-3-carboxamide), has been shown to exhibit a higher efficacy than ivacaftor for the G551D mutation, yet the underlying mechanism of GLPG1837 remains unclear. Here we find that despite their differences in potency and efficacy, GLPG1837 and VX-770 potentiate CFTR gating in a remarkably similar manner. Specifically, they share similar effects on single-channel kinetics of wild-type CFTR. Their actions are independent of nucleotide-binding domain (NBD) dimerization and ATP hydrolysis, critical steps controlling CFTR's gate opening and closing, respectively. By applying the two reagents together, we provide evidence that GLPG1837 and VX-770 likely compete for the same site, whereas GLPG1837 and the high-affinity ATP analogue 2'-deoxy-*N*⁶-(2-phenylethyl)-adenosine-5'-*O*-triphosphate (dPATP) work synergistically through two different sites. We also find that the apparent affinity for GLPG1837 is dependent on the open probability of the channel, suggesting a state-dependent binding of the drug to CFTR (higher binding affinity for the open state than the closed state), which is consistent with the classic mechanism for allosteric modulation. We propose a simple four-state kinetic model featuring an energetic coupling between CFTR gating and potentiator binding to explain our experimental results.

INTRODUCTION

CFTR, a member of the ATP-binding cassette (ABC) protein superfamily, is unique in that instead of being a transporter, CFTR is a chloride channel that plays a critical role in the regulation of water and salt movement across epithelium-lining tissues (Riordan et al., 1989; Quinton and Reddy, 1991; Bear et al., 1992). Loss-of-function mutations in the *CFTR* gene are the root cause of the lethal hereditary disease cystic fibrosis (CF), affecting one in every ~2,500 newborns of Caucasian origin (Zielenski and Tsui, 1995; Rowe et al., 2005). Recently, the breakthrough in solving the atomic structure of human CFTR protein provided the first glimpse of the fundamental features of this channel at a molecular level (Liu et al., 2017). Like most ABC transporters, CFTR inherits two transmembrane domains (TMDs) that craft the chloride permeation pathway and two cytosolic nucleotide-binding domains (NBD1 and NBD2), where CFTR's ligand ATP binds to gate the channel. In addition, CFTR possesses a unique

regulatory (R) domain containing multiple serine residues for PKA-dependent phosphorylation (Ostedgaard et al., 2001). Once the R domain is phosphorylated, the gating cycle of CFTR is driven by ATP binding-induced NBD dimerization and hydrolysis-elicited partial separation of the NBD dimer (Vergani et al., 2003, 2005; Hwang and Sheppard, 2009; Tsai et al., 2009, 2010; Chaves and Gadsby, 2015).

Approximately 2,000 different mutations have been identified (<http://www.genet.sickkids.on.ca/cftr/>) since the first cloning of the *CFTR* gene in 1989 (Riordan et al., 1989). Currently, disease-associated mutations are grouped into six classes based on their defective mechanisms (Welsh and Smith, 1993; Zielenski and Tsui, 1995; Rowe et al., 2005; Veit et al., 2016). The most prevalent mutation, the deletion of phenylalanine at position 508 ($\Delta F508$), results in both severe folding (Du et al., 2005; Thibodeau et al., 2005; Cui et al., 2007; Rosser et al., 2008; Du and Lukacs, 2009) and gating (Dalemans et al., 1991; Hwang et al., 1997; Cui et al., 2006) defects. On the other hand, the third most common disease-associated

Correspondence to Tzyh-Chang Hwang: hwangt@health.missouri.edu

Abbreviations used: CF, cystic fibrosis; dPATP, 2'-deoxy-*N*⁶-(2-phenylethyl)-adenosine-5'-*O*-triphosphate; GLPG1837, *N*-(3-carbamoyl-5,5,7,7-tetramethyl-4,7-dihydro-5*H*-thieno[2,3-*c*]pyran-2-yl)-1*H*-pyrazole-3-carboxamide; NBD, nucleotide-binding domain; NPPB, 5-nitro-2-(3-phenylpropylamino)benzoate; TMD, transmembrane domain; VX-770, *N*-(2,4-di-tert-butyl-5-hydroxyphenyl)-4-oxo-1,4-dihydroquinoline-3-carboxamide.

© 2017 Yeh et al. This article is distributed under the terms of an Attribution-Noncommercial-Share Alike-No Mirror Sites license for the first six months after the publication date (see <http://www.rupress.org/terms/>). After six months it is available under a Creative Commons License (Attribution-Noncommercial-Share Alike 4.0 International license, as described at <https://creativecommons.org/licenses/by-nc-sa/4.0/>).



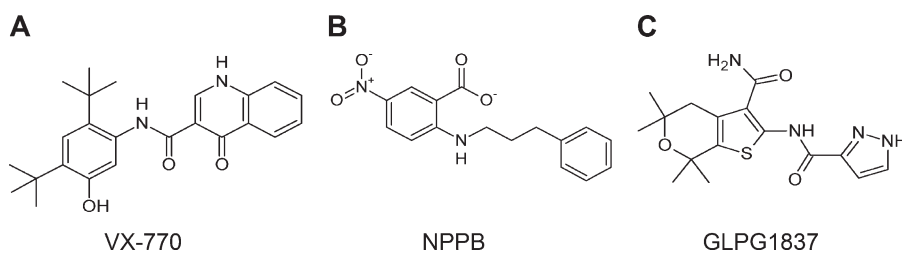


Figure 1. Comparison of chemical structures of CFTR potentiators. (A–C) Chemical structures of VX-770 (A), NPPB (B), and GLPG1837 (C) as marked.

mutation, G551D, primarily impairs channel gating, reducing the open probability (P_o) by more than 100-fold (Welsh and Smith, 1993; Cai et al., 2006; Bompadre et al., 2007). In the past few decades, tremendous efforts have been made to develop compounds targeting the CFTR protein itself. Those CFTR modulators that can increase the P_o of CFTR are known as CFTR potentiators (Hwang and Sheppard, 1999; Rowe and Verkman, 2013; Barry et al., 2015; Jih et al., 2017). Among the plethora of CFTR potentiators, however, only a few have been extensively investigated. Based on their mechanisms of action, these well-studied reagents can be classified into three major groups: (1) ATP analogues that target the ATP-binding sites, such as N^6 -(2-phenylethyl)-ATP (PATP; Zhou et al., 2005; Bompadre et al., 2008; Tsai et al., 2010), 2'-deoxy-ATP (dATP; Aleksandrov et al., 2002; Cai et al., 2006), and 2'-deoxy- N^6 -(2-phenylethyl)-adenosine-5'-*O*-triphosphate (dPATP; Miki et al., 2010); (2) compounds that are proposed to work on the TMDs to stabilize the open channel configuration, including nitrate (Yeh et al., 2015) and *N*-(2,4-di-tert-butyl-5-hydroxyphenyl)-4-oxo-1,4-dihydroquinoline-3-carboxamide (VX-770; Fig. 1 A; Van Goor et al., 2009; Eckford et al., 2012; Jih and Hwang, 2013); and (3) 5-nitro-2-(3-phenylpropylamino)benzoate (NPPB; Fig. 1 B; Wang et al., 2005), which appears to promote gate opening with unsettled mechanisms (Csanády and Töröcsik, 2014; Lin et al., 2016).

The FDA's approval of VX-770 for the treatment of CF in 2012 ushered in a new era of personalized medicine in CF. Although the original application of VX-770 was limited to patients carrying the G551D mutation, now it is used for a broad spectrum of mutations because *in vitro* studies showed that VX-770 potentiates the activity of a variety of CFTR mutants with gating abnormalities (Yu et al., 2012; Van Goor et al., 2014). One potential downside with VX-770 as a therapeutic reagent is that prolonged exposure of VX-770 may have negative impacts on the action of VX-809 (Cholon et al., 2014; Veit et al., 2014), a CFTR corrector designed to ameliorate the trafficking defect associated with the $\Delta F508$ mutation (Van Goor et al., 2011). In addition, the VX-770-treated G551D channels have a P_o still less than 10% of that of WT channels (Jih and Hwang, 2013; but compare Van Goor et al., 2009). Therefore, developing new CFTR potentiators with improved pharmacological properties remains an important goal.

Lately, a novel and potentially more effective CFTR potentiator, *N*-(3-carbamoyl-5,5,7,7-tetramethyl-4,7-dihydro-5*H*-thieno[2,3-*c*]pyran-2-yl)-1*H*-pyrazole-3-carboxamide (GLPG1837; Fig. 1 C), was identified by Conrath et al. (2016. The 30th Annual North American Cystic Fibrosis Conference. Poster 23) using a YFP-based high-throughput screening assay. In the current study, we demonstrate that although it has a chemical structure different from VX-770 (compare Fig. 1, A and C), GLPG1837 may share a common mechanism with VX-770 in modulating CFTR functions by binding to the same site. Our data also show a P_o -dependent shift of the dose–response relationships for GLPG1837—the lower the P_o , the higher the concentration required for reaching 50% of the maximal effect ($K_{1/2}$), a phenomenon that can be explained by state-dependent binding. We therefore propose a classic allosteric model featuring an energetic coupling between binding of GLPG1837 and gating. Computer simulations using this simple model can indeed replicate most of our data.

MATERIALS AND METHODS

Cell culture and transfection

Chinese hamster ovary (CHO) cells were used for all patch-clamp experiments. CHO cells were grown at 37°C in Dulbecco's modified Eagle's medium supplemented with 10% (vol/vol) FBS. 1 d before the transfection, cells were trypsinized and transferred to 35-mm tissue culture dishes. We performed transfection with pcDNA plasmids carrying different CFTR constructs and green fluorescence protein encoding pEGFP-C3 (Takara Bio) by using PolyFect transfection reagent (Qiagen). After transfection, cells were incubated at 27°C for 2–3 d before experiments for microscopic current recordings and 3–6 d for macroscopic current recordings.

Mutagenesis

CFTR mutants were constructed using QuikChange XL kit (Agilent) according to the manufacturer's protocol. All DNA constructs were sequenced by the DNA Core Facility (University of Missouri, Columbia, MO) to confirm the mutation identity.

Electrophysiological recordings

In patch-clamp experiments, glass chips carrying the transfected cells were transferred to a chamber lo-

cated on the stage of an inverted microscope (IX51; Olympus). A two-stage micropipette puller (PP-81; Narishige) was used to pull borosilicate capillary glasses into patch pipettes, which were then polished with a homemade microforge to a resistance of 2–4 M Ω in the bath solution. Membrane patches were excised to an inside-out configuration once a seal resistance >40 G Ω was reached. Subsequently, the pipette tip was placed to the outlet of a three-barrel perfusion system and perfused with 25 IU PKA and 2 mM ATP until the current reached a steady state. To maintain the phosphorylation level of the CFTR channels, 6 IU PKA was added to all other ATP-containing solutions applied thereafter. All electrophysiological data were recorded with a patch-clamp amplifier (EPC9; HEKA) at room temperature. An eight-pole Bessel filter (LPF-8; Warner Instruments) was used to filter the data at 100 Hz and digitized to a computer at a sampling rate of 500 Hz. For macroscopic and single-channel recordings, the membrane potential was held at –30 and –50 mV, respectively. Solution changes were effected with a fast solution change system (SF-77B; Warner Instruments) with a dead time of ~30 ms (Tsai et al., 2009).

Of note, the effect of VX-770 cannot be washed out by a continuous perfusion of VX-770-free solution within the experimentally permissible time. As a result, we could not bracket our experiments with this reagent. Instead, all experiments with VX-770 were done after first obtaining a control in the same patch. All devices that had been in contact with VX-770 were repeatedly washed with 50% DMSO to minimize contamination by residual VX-770.

Chemicals and solution compositions

For all of the patch-clamp experiments, pipette solution contained (mM) 140 NMDG-Cl, 5 CaCl₂, 2 MgCl₂, and 10 HEPES, pH 7.4 with NMDG. Cells were perfused with a bath solution containing (mM) 145 NaCl, 2 MgCl₂, 5 KCl, 1 CaCl₂, 5 glucose, 5 HEPES, and 20 sucrose, pH 7.4 with NaOH, before patch excision. After an inside-out configuration was established, the patch was perfused with a standard perfusion solution containing (mM) 150 NMDG-Cl, 2 MgCl₂, 1 CaCl₂, 10 EGTA, and 8 Tris, pH 7.4 with NMDG.

PKA and MgATP were purchased from Sigma-Aldrich. MgATP was stored in 500 mM stock solutions at –20°C. The [MgATP] used in this study was 2 mM unless otherwise indicated in the figures. dPATP was custom-synthesized by Biolog Life Science Institute and stored in 10-mM stock solutions at –70°C. VX-770, provided by R. Bridges (Rosalind Franklin University, North Chicago, IL), was stored as a 100- μ M stock in DMSO at –70°C. GLPG1837 was provided by Galapagos and stored as a 10-mM stock at –20°C. All chemicals were diluted to the concentrations indicated in each figure

with the perfusion solution, and the pH was adjusted to 7.4 with NMDG.

Data analysis and statistics

Igor Pro program (Wave-Metrics) was used to measure the steady-state mean current amplitude and estimate the relaxation time constant. The current decay upon removal of ATP, dPATP, or GLPG1837 were fitted with built-in single or double exponential functions to obtain the relaxation time constants. Single-channel kinetic analysis was done with a program developed by Csanády (2000), which allows microscopic kinetic analysis for recordings containing fewer than eight openings. We took a more conservative approach to analyze only traces with less than four opening steps for all the microscopic experiments. The partition coefficients and log P values were calculated by using ACD/ChemSketch (www.acdlabs.com). Student's t tests assuming equal variance were conducted with Excel for the comparisons showing statistical probability. Paired t test was conducted for analysis in Figs. 4 B and 7 D and Fig. S3 B. $P < 0.05$ was considered statistically significant. The error bars represent SEM in all figures.

Online supplemental material

Fig. S1 shows raw traces of locked-open events occasionally observed with WT-CFTR potentiated by GLPG1837. Figs. S2 and S3 present additional enhancement of G551D-CFTR currents by nitrate in the presence of dPATP plus GLPG1837. Fig. S4 demonstrates the effect of GLPG1837 on WT-CFTR in the absence of ATP. Figs. S5 and S6 are simulated results for data shown in Figs. 2 and 7, respectively. Table S1 lists the parameters used in the simulations. The online supplemental material also includes discussion on the limitations and possible alternatives for the allosteric modulation model proposed in Fig. 10.

RESULTS

As a first step to characterize GLPG1837, we examined the effect of acute addition of this compound to macroscopic WT-CFTR currents preactivated with PKA and ATP to a steady state at a holding potential of –30 mV in excised inside-out patches. Fig. 2 A shows a representative real-time recording in which an application of 3 μ M GLPG1837 in the continuous presence of ATP enhances the currents by 2.06 ± 0.08 -fold ($n = 19$). This potentiation effect is reversible and concentration dependent. The dose responses at different concentrations of GLPG1837 were normalized to the currents at 3 μ M GLPG1837 in the same patch, and the data can be fitted with the Hill equation, yielding a $K_{1/2}$ of 0.23 ± 0.12 μ M and a Hill coefficient of 0.70 ± 0.24 (Fig. 2 B).

Interestingly, when we closely examined the macroscopic current relaxations upon removal of ATP in the

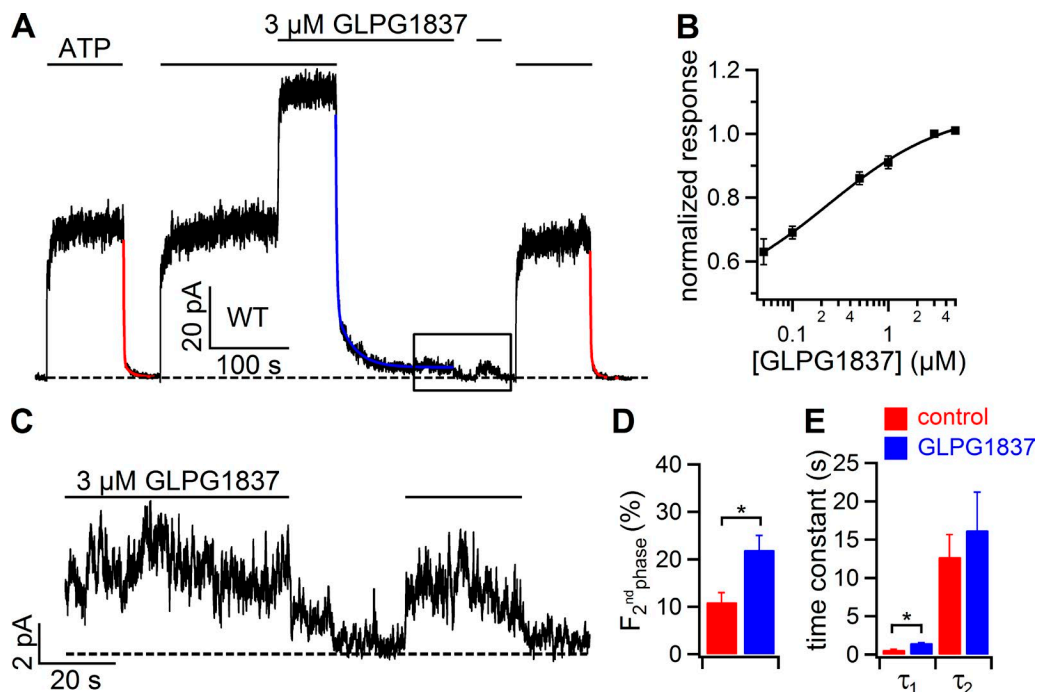


Figure 2. Effects of GLPG1837 on ATP-dependent and ATP-independent gating of WT-CFTR. (A) A continuous macroscopic current trace of WT-CFTR showing the responses to GLPG1837 in the presence or absence of ATP. In an inside-out patch containing WT-CFTR channels preactivated with 2 mM ATP plus PKA, we applied 2 mM ATP until a steady-state current was attained. Subsequent removal of ATP results in a current decay to the baseline. The overlapping red line indicates double exponential fit of the current drop. After the current was brought back to the level achieved by ATP, an additional application of 3 μ M GLPG1837 increased the current by approximately twofold (2.06 ± 0.08 , $n = 19$). In the continuous presence of GLPG1837, the current decays upon removal of ATP, but a significant residual current can be seen. The blue line marks a double exponential fit of the current decay. For the residual, ATP-independent current, removal of GLPG1837 leads to a further current decrease (rectangular box). Bars above the trace mark the duration of applications of the indicated reagents. (B) Dose–response curve of GLPG1837 for WT-CFTR. The currents potentiated by different concentrations of GLPG1837 were normalized to the one at 3 μ M GLPG1837 in the same patch. The dose-dependent effects were fitted with the Hill equation, yielding a $K_{1/2}$ of 0.23 ± 0.12 μ M and a Hill coefficient of 0.70 ± 0.24 . Each data point represents values determined from three to seven patches. (C) Magnification of the rectangular boxed area in A. In the absence of ATP, GLPG1837 reversibly enhances channel activity. (D) Fraction of the second phase of the current relaxation upon ATP washout in the absence (red) and presence (blue) of GLPG1837. (E) Relaxation time constants for the current decay upon ATP washout. τ_1 represents the fast first phase, and τ_2 the slow second phase, of double-exponential fitting. Error bars represent SEM. *, $P < 0.05$.

absence or presence of GLPG1837, a striking difference emerged. The current decline after washout of ATP in the absence of GLPG1837 can be well fitted with a double-exponential function, with 90% of the current decay within the first fast phase (Fig. 2 A, red line). However, in the presence of GLPG1837, removal of ATP shows a visually distinguishable slow phase in addition to the fast phase (Fig. 2 A, blue line). In addition, the residual currents in the continuous presence of GLPG1837 remain discernable for hundreds of seconds even in a solution without ATP (Fig. 2 A, boxed area). Fig. 2 C magnifies the boxed area in Fig. 2 A, highlighting that the residual currents long after ATP removal can be reversibly potentiated by GLPG1837. Fig. 2 (D and E) summarizes the parameters of double-exponential curve fitting for the current relaxations upon ATP washout. The fraction of second phase in the presence of GLPG1837 is significantly larger than that in the absence of GLPG1837 ($22 \pm 3\%$ and $11 \pm 2\%$, respectively; $n = 7$; $P < 0.05$). Of note,

because the ATP-induced currents in the presence of GLPG1837 are approximately twofold larger than the control, the twofold increase of the second fraction by GLPG1837 indicates that the initial current after the completion of the fast-phase current drop is increased by fourfold with GLPG1837. In addition, the relaxation time constant of the fast current decay (τ_1) is prolonged by GLPG1837 ($\tau_1 = 1.51 \pm 0.36$ s with GLPG1837; $\tau_1 = 0.62 \pm 0.08$ s without GLPG1837; $n = 7$; $P < 0.05$), whereas the time constants of the second phase (τ_2) are not significantly different. These observations led us to conclude that GLPG1837 potentiates both ATP-dependent and ATP-independent gating of WT-CFTR.

We next tested the effects of GLPG1837 on WT-CFTR in patches containing fewer than four channels to understand the kinetic effects of GLPG1837. As shown in Fig. 3 A, single-channel activity of WT-CFTR was recorded in the same patch either with or without the application of GLPG1837. The open time is indeed visibly

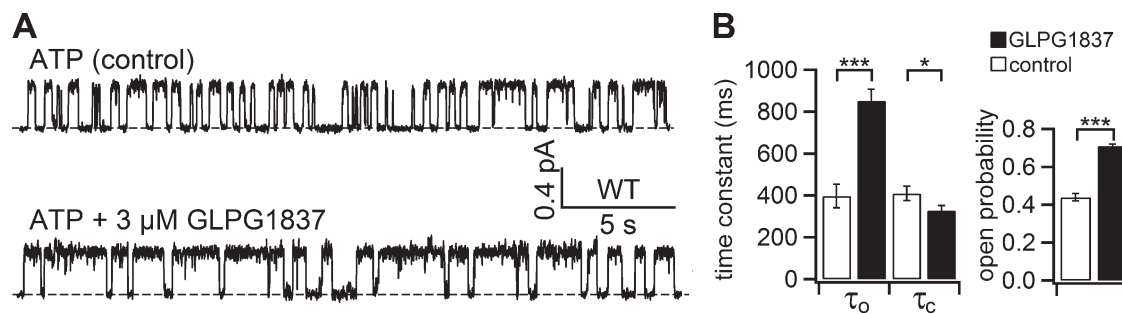


Figure 3. Effects of GLPG1837 on single-channel kinetics of WT-CFTR. (A) Representative single-channel recordings of WT-CFTR in the absence (top trace) or presence (bottom trace) of 3 μ M GLPG 1837. WT-CFTR in an inside-out patch was activated by PKA plus 2 mM ATP before the solution was switched to one with 2 mM ATP only. The dashed line represents the current level when the channel is closed. (B) Kinetic parameters of WT-CFTR in the absence (blank bar) or presence (filled bar) of GLPG1837. τ_o , open time constant; τ_c , closed time constant; P_o : 397 \pm 56 ms, 409 \pm 35 ms, 0.44 \pm 0.02 without GLPG1837 (n = 7); 851 \pm 55 ms, 328 \pm 24 ms, 0.71 \pm 0.01 with GLPG1837 (n = 9). Error bars represent SEM. *, P < 0.05; ***, P < 0.001.

longer in the GLPG1837 than in its absence. Fig. 3 B summarizes results from single-channel kinetic analysis and confirms an increase of the P_o by GLPG1837 (0.71 \pm 0.01 and 0.44 \pm 0.02 with and without GLPG1837, n = 9 and n = 7, respectively; P < 0.001). Although the mean closed time constant (τ_c) is slightly decreased, GLPG1837 predominantly increases the P_o by prolonging the open time constant (τ_o) from 397 \pm 56 ms (n = 7) to 851 \pm 55 ms (n = 9; P < 0.001). Comparing the macroscopic and microscopic data, we noticed a discrepancy between the predicted P_o estimated by macroscopic current fold increase (\sim 0.9) and the actual P_o measured from microscopic kinetic analysis (0.71). Fig. S1 provides a possible explanation. In short, in the single-channel recording in the presence of GLPG1837, we occasionally observed long opening events that lasted for tens to hundreds of seconds even after ATP was removed from the solution (Fig. S1, A and B), also known as the locked-open phenomenon (Gunderson and Kopito, 1994). It is noteworthy that these locked-open events, rarely observed in WT channels gated with ATP alone, were seen more often in the presence of GLPG1837. Because we excluded the locked-open events in microscopic kinetic analysis, the P_o was inevitably underestimated, resulting in a fold increase of microscopic P_o lower than that of macroscopic currents.

Although a swath of reagents has been reported to enhance the gating function of CFTR, detailed mechanistic studies for these CFTR potentiators are limited (reviewed in Hwang and Sheppard, 1999; Rowe and Verkman, 2013; Jih et al., 2017). As described in the Introduction, we can divide the potentiators into three major categories based on their mechanisms of action: (1) ATP analogues, (2) VX-770 and nitrate, and (3) NPPB. Given that the chemical structure of GLPG1837 is distinct from ATP or its derivatives, it is unlikely that GLPG1837 works via the same mechanism as ATP analogues. However, whether the action of GLPG1837 is distinct from any other potentiators remains unclear.

One unique pharmacological property distinguishing NPPB from VX-770 is that the current relaxation upon removal of ATP for hydrolysis-deficient mutants was shortened by NPPB (Lin et al., 2016) but prolonged by VX-770 (Kopeikin et al., 2014). We reasoned that this opposite effect on nonhydrolytic closing may serve as a tool to distinguish whether GLPG1837 works similarly to VX-770 or NPPB. Therefore, we tested the effects of GLPG1837 on the nonhydrolytic closing rate of E1371S-CFTR, a hydrolysis-deficient mutant whose ATPase activity was abolished by replacing the catalytic glutamate with a serine (Stratford et al., 2007). Fig. 4 A shows that the relaxation time constant upon removal of ATP in the absence of GLPG1837 can be fitted with a single-exponential function with a time constant of \sim 50 s (red line), which was greatly prolonged to \sim 103 s (blue line) in the presence of GLPG1837, suggesting that GLPG1837 decelerates nonhydrolytic closing of the channels. The relaxation time constants are summarized in Fig. 4 B.

This effect of GLPG1837 on nonhydrolytic closing was further confirmed in another hydrolysis-deficient mutant, D1370N/ Δ R-CFTR (Csanády et al., 2010), which allows examinations of microscopic kinetics. As seen in Fig. 4 C, the P_o of D1370N/ Δ R-CFTR is \sim 0.5 at 2 mM ATP; the opening bursts of D1370N/ Δ R-CFTR are visibly prolonged by GLPG1837 in single-channel recordings. Of note, this set of experiments was performed in the Δ R background, which bears two distinct advantages: first, the experiments can be performed immediately after excising the patch without phosphorylation, and hence any dephosphorylation-induced effects are avoided; second, the reduced expression of the Δ R construct facilitates acquisition of single-channel data. In the presence of GLPG1837, the opening bursts for D1370N/ Δ R-CFTR are lengthened to 1659 \pm 295 ms (vs. 930 \pm 143 ms in control; P < 0.05), and the inter-burst durations are considerably shortened from 694 \pm 125 to 200 \pm 39 ms, resulting in a P_o of 0.87 \pm 0.02 (n =

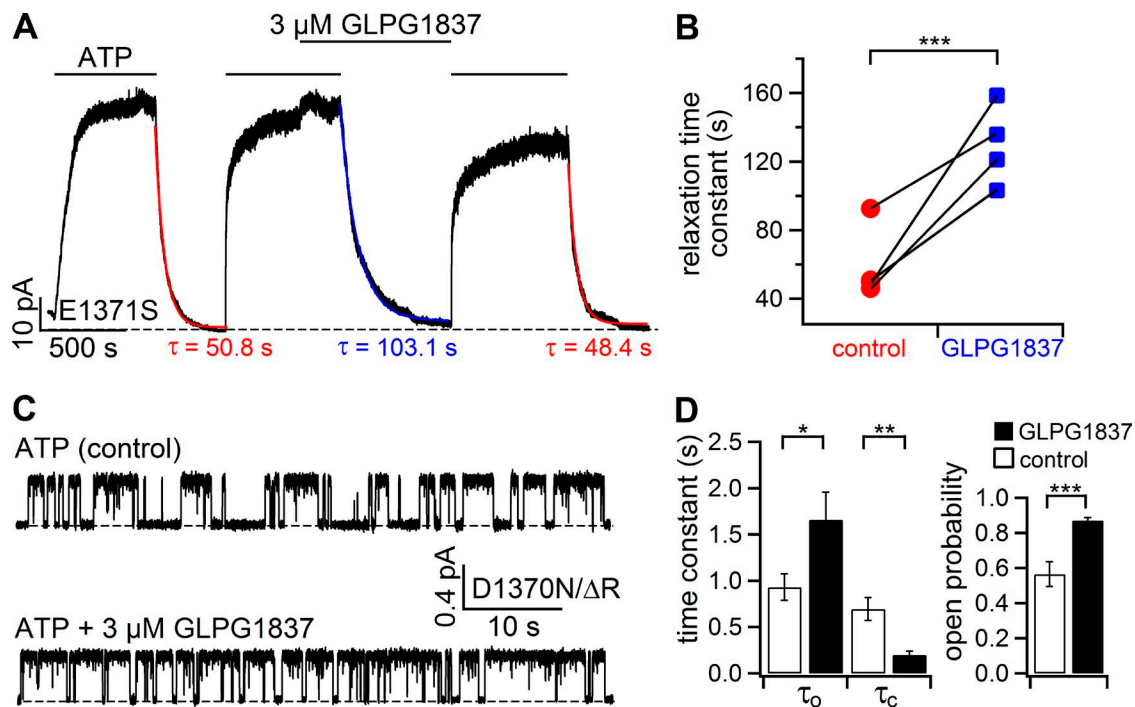


Figure 4. **Effects of GLPG1837 on hydrolysis-deficient mutants.** (A) GLPG1837 decelerates nonhydrolytic closing of E1371S-CFTR. Macroscopic currents of E1371S-CFTR were activated by PKA and 2 mM ATP, and the subsequent removal of ATP resulted in a current decay, yielding a relaxation time constant of 50.8 s when fitted with a single exponential function (red line). In the presence of 3 μ M GLPG1837, the relaxation time constant was prolonged to 103.1 s (blue line). (B) Comparison of the relaxation time constants for E1371S-CFTR with and without GLPG1837. Each pair of time constants (linked by a straight line) was obtained from experiments done in the same patch as the example in A. (C) Modulation of D1370N/ Δ R-CFTR gating by GLPG1837. (D) Microscopic kinetic parameters for D1370N/ Δ R-CFTR. P_o , τ_o , and τ_c : 0.57 ± 0.07 , 930 ± 143 ms, and 694 ± 125 ms in the absence of GLPG1837 ($n = 4$); 0.87 ± 0.02 , 1659 ± 295 ms, and 200 ± 39 ms in its presence ($n = 5$). Error bars represent SEM. *, $P < 0.05$; **, $P < 0.01$; ***, $P < 0.001$.

5, Fig. 4 D). Thus, data presented in Fig. 4 suggest that GLPG1837 may work differently than NPPB.

We next considered the possibility that GLPG1837 shares a similar mechanism of action with VX-770. Our current understanding for the action of VX-770 can be summarized in three major features: first, VX-770 increases both ATP-dependent and ATP-independent gating of CFTR (Eckford et al., 2012; Jih and Hwang, 2013); second, VX-770 slows down nonhydrolytic closing (Jih and Hwang, 2013; Kopeikin et al., 2014); third, VX-770 potentiates mutants with defective NBD dimerization such as G551D-CFTR (Van Goor et al., 2009; Yu et al., 2012) and Δ NBD2-CFTR (Yeh et al., 2015), presumably by perturbing the equilibrium between closed- and open-channel configurations in the TMDs (Jih and Hwang, 2013). Our experimental data of GLPG1837 presented so far match the first two features of VX-770. We therefore asked whether GLPG1837 acts on G551D-CFTR and Δ NBD2-CFTR as well.

Fig. 5 A shows that 3 μ M GLPG1837 dramatically increases the currents of G551D-CFTR by ~ 20 -fold (19.85 ± 0.94 -fold increase, $n = 27$). The maximal current increase at the saturating concentration of GLPG1837 (20 μ M) reaches 35.62 ± 5.42 -fold, which is larger than the maximal effect of VX-770 (~ 6 -fold

increase of P_o , as shown in Van Goor et al., 2009, but ~ 10 -fold in Jih and Hwang, 2013). Interestingly, the biphasic current decay after ATP washout in the continuous presence of GLPG1837 was also seen with G551D-CFTR potentiated with VX-770, as reported in Lin et al. (2014). Subsequent removal of GLPG1837 results in further current decay, supporting the idea that GLPG1837 exerts its effects even in the absence of ATP. Inh-172 (Ma et al., 2002; Kopeikin et al., 2010) was applied at the end of the recording to ensure the consistence of the baseline. We further demonstrated that the response to GLPG1837 is independent of the formation of dimeric NBDs by treating Δ NBD2-CFTR with GLPG1837 (Fig. 5 B). The effectiveness of GLPG1837 on Δ NBD2-CFTR also reiterates the idea that GLPG1837 and NPPB work via different mechanisms, as deletion of NBD2 drastically reduces the efficacy of NPPB (Lin et al., 2016). Fig. 5 C depicts the dose-response relationships of GLPG1837 for G551D-CFTR and Δ NBD2-CFTR. Fitting of the Hill equation yields $K_{1/2}$ values of 2.23 ± 0.25 and 1.19 ± 0.03 μ M, respectively. It is interesting to note that the $K_{1/2}$ values of G551D-CFTR and Δ NBD2-CFTR are ~ 10 -fold higher than that of WT-CFTR (0.23 ± 0.12 μ M; black curve in Fig. 5 C). This finding prompted us to com-

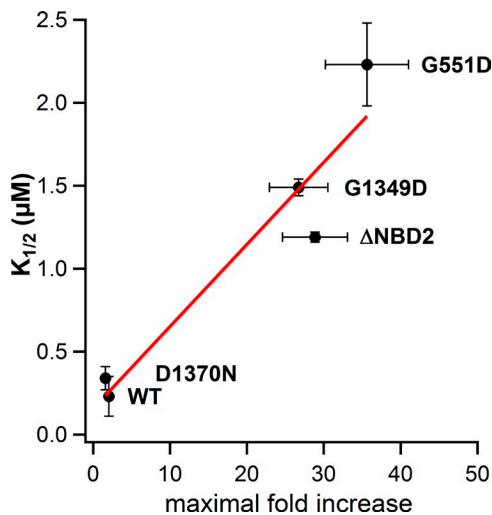


Figure 6. Positive correlation between the apparent affinities of GLPG1837 and the maximal fold increase of macroscopic currents for five different CFTR constructs treated with GLPG1837. The data were obtained from the dose–response experiments described in the previous figures (Figs. 2 B and 5 C) and fitted with a linear line with an R^2 of 0.90. Error bars represent SEM.

pare the $K_{1/2}$ for GLPG1837 for mutants that exhibit similar gating defects, such as G1349D-CFTR ($K_{1/2} = 1.49 \pm 0.05 \mu\text{M}$), and a mutation that does not alter the P_o , D1370N-CFTR ($K_{1/2} = 0.34 \pm 0.07 \mu\text{M}$). It appears that the dose–response curves are rightward-shifted in G551D-, ΔNBD2 -, and G1349D-CFTR compared with WT- and D1370N-CFTR. The fundamental difference between the two groups (G551D-, ΔNBD2 -, and G1349D-CFTR vs. WT- and D1370N-CFTR) is that the former has severe gating defects leading to a reduction of the P_o (Cai et al., 2006; Bompadre et al., 2007; Miki et al., 2010), which is reflected by a large current fold increase upon application of GLPG1837, whereas D1370N-CFTR assumes a P_o (Gunderson and Kopito, 1995) similar to that of WT channels, and the maximal current increase of both channels is only ~ 2 -fold (2.06 ± 0.08 -fold for WT-CFTR and 1.59 ± 0.36 -fold for D1370N-CFTR). As we plotted the relationship between maximal fold increase and $K_{1/2}$ of GLPG1837, a positive correlation emerged (Fig. 6; $R^2 = 0.90$). This finding raised the possibility that the apparent affinity of GLPG1837 may be a function of the P_o of the channels: the lower the P_o (i.e., the higher the maximal fold increase in P_o), the lower the affinity.

One caveat in relating the P_o and the apparent affinity of GLPG1837 (Fig. 6) is that different CFTR constructs were used; thus one cannot exclude the effects of mutation itself on the measured $K_{1/2}$. Nonetheless, the hypothesis that the affinity of GLPG1837 is determined by the P_o of the channels predicts two scenarios. First, if we performed the dose–response experiments on a channel whose P_o has already been raised to a higher level

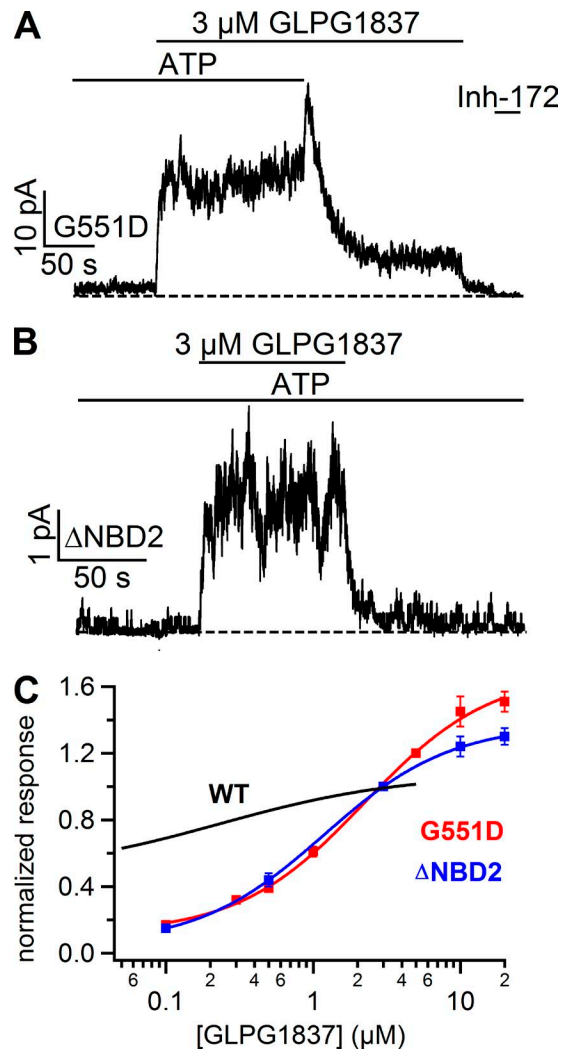


Figure 5. GLPG1837 potentiates the activity of CFTR mutants with defective NBD dimerization. (A) Effects of GLPG1837 on G551D-CFTR. PKA-phosphorylated G551D-CFTR currents in the presence of 2 mM ATP increased by 19.85 ± 0.94 -fold ($n = 27$) upon the application of $3 \mu\text{M}$ GLPG1837. Washout ATP in the continuous perfusion of GLPG1837 resulted in a biphasic current decay, presumably caused by a fast release of ATP inhibition in site 2 followed by a slower dissociation of ATP from site 1 (Lin et al., 2014). The subsequent removal of GLPG1837 caused a further decrease of the current, with the residual current inhibited by $5 \mu\text{M}$ Inh-172. (B) Effects of GLPG1837 on ΔNBD2 -CFTR. In the presence of 2 mM ATP, $3 \mu\text{M}$ GLPG1837 increased the currents of ΔNBD2 -CFTR by 21 ± 1.5 -fold ($n = 12$). (C) Dose–response relationships of GLPG1837 for G551D- and ΔNBD2 -CFTR. The experimental data at different concentrations of GLPG1837 were normalized to the current at $3 \mu\text{M}$ GLPG1837. Fitting parameters for G551D: $K_{1/2} = 2.23 \pm 0.25 \mu\text{M}$; Hill coefficient (n) = 1.01 ± 0.12 ; for ΔNBD2 : $K_{1/2} = 1.19 \pm 0.03 \mu\text{M}$ and $n = 1.01 \pm 0.02$. The black curve represents the dose–response curve for WT channels in Fig. 2 B. Error bars represent SEM.

by a different class of potentiators, the dose–response curve should be shifted to the left. Second, if we lower the P_o of WT channels by decreasing the concentration

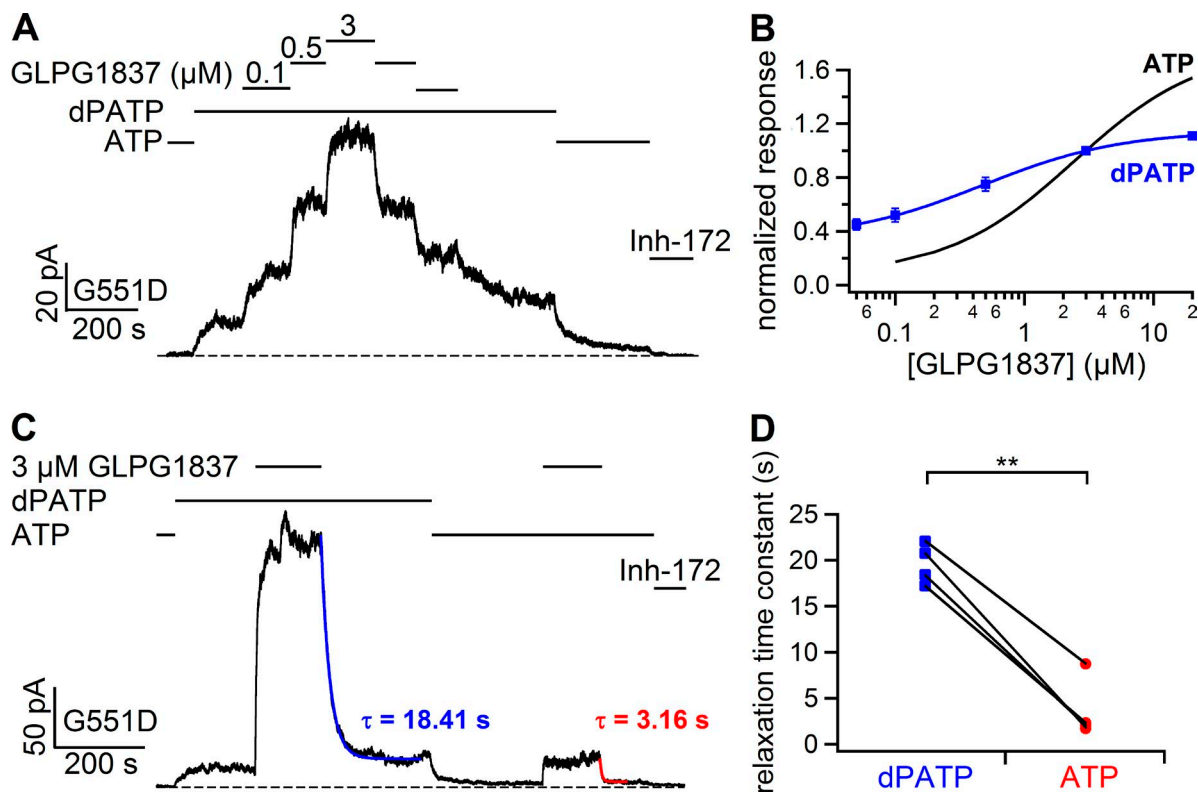


Figure 7. Increasing the apparent affinity of GLPG1837 by manipulating P_o of G551D-CFTR. (A) Dose–response of GLPG1837 on G551D-CFTR gated by dPATP. Once the currents had reached the steady state, 2 mM ATP was replaced by 20 μ M dPATP, resulting in a 17.43 ± 1.28 -fold current increase ($n = 17$). The following applications of GLPG1837 at different concentrations are marked above the trace. (B) Leftward shift of the dose–response relationship of GLPG1837 as the P_o of G551D-CFTR increases. Hill equation fitting parameters: $K_{1/2} = 0.47 \pm 0.02 \mu\text{M}$ and Hill constant = 0.81 ± 0.03 for channels gated by 20 μ M dPATP. The black curve is obtained from Fig. 5 C at 2 mM ATP. Data points represent the mean values from 3–12 patches and were normalized to the current level at 3 μ M GLPG1837 in the same patch. (C) A comparison of G551D-CFTR current relaxation upon removal of GLPG1837 in conditions as indicated. Currents were first potentiated by 20 μ M dPATP, and an additional application of 3 μ M GLPG1837 further increased the currents. The subsequent removal of GLPG1837 resulted in a current decay, which was fitted with a single-exponential function with a time constant of 18.41 s (blue fitted curve), which was shortened to 3.16 s when dPATP was replaced with 2 mM ATP (red fitted curve). (D) Diagram summarizing the relaxation time constants in four different patches under the indicated conditions. Each pair represents data obtained from the same patch. **, $P < 0.01$.

of ATP, we should obtain a rightward-shifted dose–response relationship.

To test the first scenario, we conducted dose–response experiments on G551D-CFTR that had been exposed to a high-affinity ATP analogue, dPATP (Miki et al., 2010). Fig. 7 A shows that 20 μ M dPATP potentiates G551D currents by 17.43 ± 1.28 -fold ($n = 17$; Miki et al., 2010). The currents can be further enhanced by GLPG1837 in a dose-dependent manner, with a $K_{1/2}$ of $0.47 \pm 0.02 \mu\text{M}$ (Fig. 7 B). Thus, when the P_o of G551D-CFTR is increased by dPATP, the apparent affinity for GLPG1837 also increases. It should be noted that the dose–response shift is not caused by a saturation of the currents by dPATP plus GLPG1837, as Fig. S2 shows that the G551D-CFTR currents in the presence of saturating concentrations of dPATP and GLPG1837 can be further enhanced by nitrate.

Further evidence that dPATP increases the apparent affinity of GLPG1837 comes from experiments that as-

sess the apparent off-rate of GLPG1837 upon washout of the reagent. Fig. 7 C shows that the current relaxation upon removal of GLPG1837 in the presence of dPATP has a time constant of 18.4 s, which is shortened to 3.2 s when dPATP is replaced with ATP. The time constants in both conditions are summarized in Fig. 7 D ($n = 4$; $P < 0.01$). Of note, the dissociation of dPATP is decelerated by GLPG1837 as well. Fig. S3 A shows an experimental protocol similar to that of Fig. 7 C except that the current relaxation upon removal of dPATP was better fitted with a double-exponential function. Both the first (τ_1) and second (τ_2) time constants are prolonged to 10.8 and 178.4 s (blue line) in the presence of GLPG1837 ($\tau_1 = 4.5$ s and $\tau_2 = 62.4$ s in the absence of GLPG1837, red line). Comparisons of both time constants are summarized in Fig. S3 B.

So far the first scenario is confirmed: the apparent affinity of GLPG1837 is higher for G551D-CFTR when its P_o has been elevated by other potentiators. We next

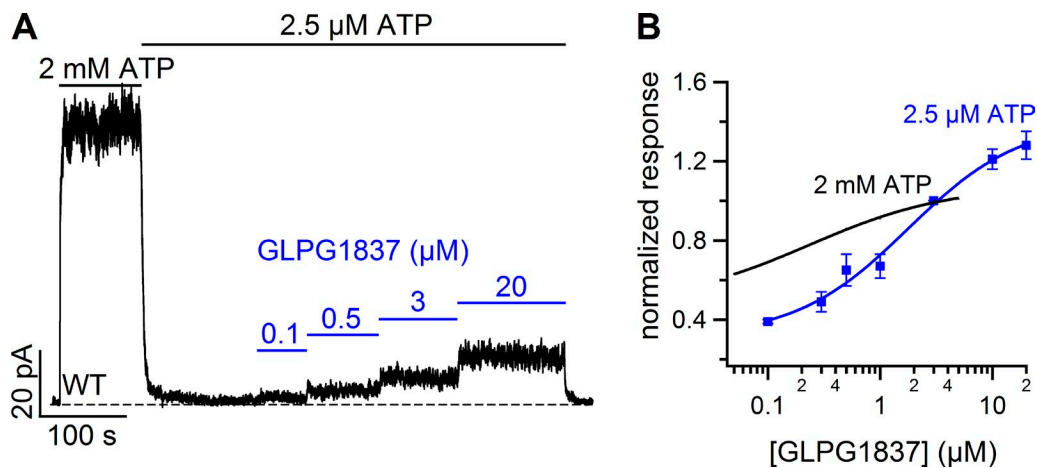


Figure 8. ***P_o*-dependent dose–response relationship of GLPG1837 in WT-CFTR.** (A) Representative current trace of dose–response experiments conducted with WT-CFTR gated by 2.5 μM ATP. Macroscopic WT current decreases as [ATP] is decreased from 2 mM to 2.5 μM. Subsequent application of GLPG1837 at various concentrations increases the current as indicated. (B) Comparison of the dose–response curves of GLPG1837 for WT-CFTR at either 2 mM (black) or 2.5 μM (blue) ATP. The rightward-shifted dose–response curve in the presence of 2.5 μM ATP is fitted with the Hill equation, yielding a $K_{1/2}$ of 1.77 ± 0.65 μM and Hill coefficient of 0.86 ± 0.35 . The black curve is obtained from Fig. 2 B. Each data point represents mean \pm SEM from 4–10 patches. Error bars represent SEM.

used WT-CFTR to test the validity of the second scenario. The idea of P_o -dependent affinity predicts that as we lower the concentration of ATP, which lowers the P_o of WT channels, we should see a decrease in the apparent affinity of GLPG1837. Indeed, Fig. 8 A shows a representative trace of dose–response experiments of GLPG1837 conducted in the presence of 2.5 μM ATP. Although 3 μM is already the saturating concentration for GLPG1837 on WT-CFTR gated by 2 mM ATP (Fig. 2 B), the current at 2.5 μM ATP, in contrast, does not saturate at such a concentration of GLPG1837. In fact, we observe a further increase of the currents upon addition of 20 μM GLPG1837, with the $K_{1/2}$ shifted to 1.77 ± 0.65 μM (Fig. 8 B, blue curve; c.f. $K_{1/2} = 0.23 \pm 0.12$ μM at 2 mM ATP), supporting our idea that the apparent affinity of GLPG1837 decreases as the P_o declines. In addition, when we completely removed ATP from the solution so that only residual currents were left, increasing [GLPG1837] from 3 to 20 μM enhanced “ATP-independent” gating of WT-CFTR (box in Fig. S4 A, expanded in Fig. S4 B). Although the current in the absence of ATP is too small to grant an accurate quantification for a complete dose–response relationship, these results echo the finding described in Fig. 8. Collectively, our data provide evidence that the apparent affinity of GLPG1837 is a function of the P_o of the channels regardless of the strategies we used to manipulate the P_o , including mutagenesis, combination of other potentiators, and changing ATP concentrations. The pharmacological and mechanistic implications will be elaborated in the Discussion.

Data presented in Fig. 7 also indicate that GLPG1837 and dPATP work through different mechanisms, as the

former can greatly enhance the G551D-CFTR currents in the presence of a saturating concentration of dPATP. This idea is perhaps not surprising because the structure of GLPG1837 (Fig. 1 C) does not resemble that of ATP. GLPG1837 is also chemically distinct from NPPB (Fig. 1 B). They do not share a common mechanism, as a decrease of the nonhydrolytic closing rate observed on E1371S-CFTR treated with GLPG1837 (Fig. 4) contradicts the effect of NPPB. Interestingly, notwithstanding the unique P_o -dependent changes in the apparent affinity of GLPG1837, the action of GLPG1837 has several features that resemble the characteristics of VX-770. They share the following similar effects as described previously: first, both ATP-dependent and -independent gating of WT-CFTR are increased (Fig. 2; Jih and Hwang, 2013); second, nonhydrolytic channel closing is decelerated (Fig. 4; Kopeikin et al., 2014); and third, gating potentiation occurs in mutants with defects in NBD dimerization (Fig. 5; Lin et al., 2014; Yeh et al., 2015). However, the fact that GLPG1837 is chemically distinguishable from VX-770 and its analogues (Hadida et al., 2014) leads us to ask how two structurally different compounds share such similarities in modulating CFTR gating.

To address this question, we tested the hypothesis that GLPG1837 and VX-770 may share a common binding site in CFTR. We reasoned that if GLPG1837 and VX-770 potentiate CFTR gating via the same binding site, occupancy of the binding site by one compound should preclude binding of the other. We chose G551D-CFTR to test this idea because the effects of both compounds have been carefully quantified on this mutant. Fig. 9 A shows a continuous recording of macroscopic G551D-

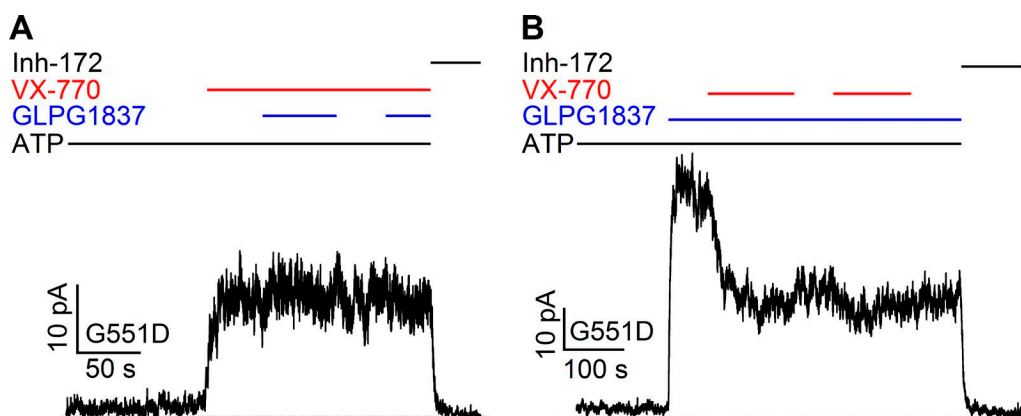


Figure 9. **GLPG1837 and VX-770 may compete for the same binding site.** (A) Macroscopic G551D-CFTR currents were first exposed to 200 nM VX-770, and subsequent addition of 3 μ M GLPG1837 failed to increase the current. Inh-172 was applied at the end of the recording to ensure an unaltered baseline. (B) G551D-CFTR currents potentiated by 3 μ M GLPG1837 were lowered by addition of VX-770 to the level achieved by VX-770 alone. Subsequent removal of VX-770 from the solution was unable to bring the current back to the original level attained by GLPG1837.

CFTR currents preactivated with PKA and ATP. The application of 200 nM VX-770 increases the currents by \sim 10-fold as expected, but more importantly, further addition of 3 μ M GLPG1837 in the presence of VX-770 fails to affect the current amplitude despite the fact that GLPG1837, when applied alone, is more efficacious than VX-770 (\sim 20-fold for GLPG1837 vs. \sim 10-fold for VX-770). On the other hand, when we reversed the protocol and applied GLPG1837 first, the currents were increased by 20-fold as expected, but the following addition of VX-770 actually lowered the current to the level equivalent to that by VX-770 alone (Fig. 9 B). Subsequent removal of VX-770 failed to bring the current back to the original level in GLPG1837. Although other more complex mechanisms can account for these results (see Supplement), the simplest explanation is that VX-770 and GLPG1837 are competing for the same site in CFTR. Of note, VX-770 assumes an extremely high affinity for CFTR (EC_{50} in the low nanomolar range, as reported in Hadida et al. [2014]); indeed, within the experimental time of tens of minutes, removal of VX-770 from the perfusate does not eliminate its effects (Jih and Hwang, 2013). Thus, if we consider the low-affinity GLPG1837 as a full agonist for the binding site, the high-affinity VX-770 is a partial agonist. The idea of competition for the same site predicts that once the binding site is occupied by the high-affinity VX-770, GLPG1837 will not be able to bind to exert its own effects on the channel because of a negligible dissociation of VX-770. In contrast, when the binding site is first taken by the low-affinity ligand GLPG1837, the high-affinity partial agonist VX-770 can replace GLPG1837. But, because of the lower efficacy of VX-770, the GLPG1837-potentiated currents are reduced gradually as more and more channels have their initial ligand substituted by VX-770.

DISCUSSION

In this study, we investigated the detailed mechanism of an alternative CFTR potentiator in development, GLPG1837, which recently has entered phase II clinical trials in patients harboring the G551D or S1251N CFTR mutation. We provide evidence that GLPG1837 shares a common mechanism for gating potentiation with VX-770 (ivacaftor), an US Food and Drug Administration–approved drug for the treatment of CF (Van Goor et al., 2009). Because the high-affinity VX-770 obviates the effects of GLPG1837, the simplest explanation for this shared mechanism is that these two reagents bind to a common binding site. In addition, our results reveal a P_o -dependent dose–response relationship for GLPG1837: the higher the P_o , the smaller the $K_{1/2}$. In this section, we first discuss the *modi operandi* of CFTR potentiators based on our current understanding of the gating mechanism of CFTR, and then use the idea of classic allostery to explain the P_o -dependent apparent affinity of GLPG1837. Finally, we speculate on the structural implications of the binding site for GLPG1837 and VX-770 based on their chemical characteristics.

It is generally accepted that once phosphorylated, opening of CFTR’s gate is coupled to ATP binding-induced NBD dimerization, and gate closure is facilitated by ATP hydrolysis-catalyzed partial (or complete) separation of the NBDs (Vergani et al., 2003, 2005; Hwang and Sheppard, 2009; Tsai et al., 2009, 2010). Although the exact mechanism by which NBD dimerization is coupled to the movement of the gate in TMDs is still debated (Sohma and Hwang, 2015), there are three critical steps involved in the gating cycle of CFTR: (1) ATP binding, (2) formation of dimeric NBDs, and (3) opening of the gate in TMDs. Therefore, any reagents that provide a favorable condition for either step could act as a CFTR

potentiator. For example, ATP analogues PATP, dATP, and dPATP increase the P_o partly because they bind better and partly because they catalyze NBD dimerization more efficiently (Aleksandrov et al., 2002; Zhou et al., 2005; Miki et al., 2010). In contrast, VX-770 is proposed to enhance CFTR functions by modulating the gating transitions between the open and closed conformations in the TMDs. Although Csanády and Töröcsik (2014) provided evidence for modulation of the transition state energy by NPPB, a CFTR potentiator that also blocks the pore (Wang et al., 2005), Lin et al. (2016) suggested that NPPB may work by facilitating NBD dimerization. Furthermore, because of the energetic coupling between NBD dimerization and gate opening (Jih et al., 2012), a synergistic but dependent interaction between NPPB and VX-770 is observed (Lin et al., 2016).

In the current study, we demonstrated two types of pharmacological interactions. On one hand, GLPG1837 and VX-770 seem to work through a competitive mechanism by which binding of one reagent precludes the effects of the other, as though they are competing for the same site. On the other hand, GLPG1837 and dPATP show a clear synergism, as even at a maximally effective concentration of dPATP, GLPG1837 can further increase the P_o of G551D-CFTR (Fig. 7 A). Moreover, the magnitude of potentiation by GLPG1837 depends on the presence or absence of dPATP. As depicted in Figs. 5 A and 7 A, 3 μ M GLPG1837 and 20 μ M dPATP cause \sim 20- and \sim 17-fold increases of G551D-CFTR currents, respectively, whereas the combined effect of both reagents is 94.55 ± 8.07 -fold ($n = 14$), which is larger than the sum of the individual effects (\sim 37-fold), indicating a pharmacological synergy (Goodman, 2011), but smaller than the value predicted if these two potentiators worked in an independent manner. (See Yeh et al. [2015], for example.)

Despite the differences in the exact kinetic steps acted on by different potentiators, one fundamental feature all potentiators must possess is that binding of the potentiators promotes channel opening. To elucidate how two separate events, channel opening and potentiator binding, are coupled, we borrowed a general four-state allosteric modulation model used successfully to explain the mechanisms of action for classical ligand-gated channels (Fig. 10 A). Based on the assumptions that ligand can bind to both the closed and open states, and that channel opening can occur whether or not the ligand is bound, this model depicts binding and gate opening as separate but coupled transitions, where the thermodynamic laws demand that if ligand binding promotes opening, then opening must promote ligand binding. It should be noted that other models that allow ligand binding only to the closed or open state may also explain state-dependent binding (see Supplement). Nevertheless, we decided to use a more generalized allosteric model, as it is less constrained.

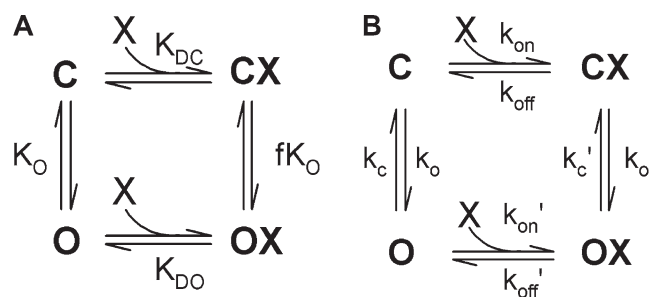


Figure 10. **Allosteric modulation model explaining the mechanism of action for classic ligand-gated channels.** (A and B) Gating scheme for ligand (X) binding and channel opening. The equilibrium constants for each step are marked in A, and the corresponding rate constants for individual transitions are indicated in B.

If we assign the equilibrium constants of gate opening/closing for the ligand-free state and ligand-bound state as K_O and fK_O , respectively, where f is greater than 1 for a ligand that increases the P_o of the channel, the opening from the ligand-bound state is more favorable than opening from the ligand-free state by a factor of f . The free energy change ($\Delta\Delta G$) needed to alter the equilibrium gating constant is $-RT\ln(f)$ kcal/mol. In a system without other sources of energy input, this $\Delta\Delta G$ then comes from a stronger binding affinity of the ligand for the channel in the open state (K_{DO}) than the closed state (K_{DC}), where K_{DC} and K_{DO} also differ by a factor of f . In other words, binding of the ligand stabilizes the open state relative to the closed state by $-RT\ln(f)$ kcal/mol.

Mathematically, this model also predicts that the apparent affinity ($K_{1/2}$) measured in the dose-response experiments should lie between K_{DC} and K_{DO} (see Supplement and Figs. S5 and S6 for details). Of note, because the P_o of G551D-CFTR is extremely low even in the presence of CFTR potentiators, the formula for P_o calculation can be simplified to k_o/k_c , where k_o and k_c represent, respectively, the opening and closing rates. Thus, the maximal macroscopic current fold increase (or efficacy) of G551D-CFTR by GLPG1837 will be approximately the same as f , which is determined by the differences of free energy of binding between the open and closed states as described in the previous paragraph. In contrast, because the measured apparent affinity from the dose-response relationship always lies between the true binding affinity of the open state and that of the closed state, the potency of GLPG1837 is determined by how tight the compound binds to the open state as well as the closed state.

The idea of state-dependent binding implies that the structure of the binding site for GLPG1837 in an open state must differ from that in a closed state, leading to different affinities. However, a maximal fold increase of \sim 35 for G551D-CFTR is equivalent to a gain

of ~ 2.1 kcal/mol of free energy for stabilizing the open state. This magnitude of $\Delta\Delta G$ can be accomplished by changes of just one hydrogen bond (Berg et al., 2002), suggesting that the binding site for GLPG1837 should not undergo a drastic structural alteration during gating. Although thermodynamic analysis only offers limited insights into the drug binding site itself, the finding that GLPG1837 and VX-770 may compete for the same site provides clues for the possible compositions of the amino acids participating in the formation of the binding pocket. Comparing the chemical structures of GLPG1837 and VX-770, we noticed that, in addition to a hydrophobic nature, they are both composed of aromatic rings linked by a peptide bond, a feature also shared by other known CFTR potentiators (Yang et al., 2003; Pedemonte et al., 2005). The exact length of the peptide bond may position the two opposing aromatic rings close to their respective binding partners that may possess aromatic and/or hydrophobic amino acids to stabilize binding. Furthermore, if, as proposed (Jih and Hwang, 2013; Yeh et al., 2015), the binding site indeed resides in the lipid–protein interface, membrane lipids should also contribute significantly to the hydrophobic interactions involved in drug binding.

Although GLPG1837 has an efficacy threefold larger than VX-770 on G551D-CFTR, its potency, reflected by the apparent affinity within a range of $0.2\sim 2$ μM (see Results for details), is much less than that of VX-770 (EC_{50} at low nanomolar range; Hadida et al., 2014). The extremely tight binding (i.e., high affinity) of VX-770 to CFTR is consistent with the observation that its effect cannot be washed out by continuous perfusion of VX-770-free solution in the experimentally permissive time frame (Jih and Hwang, 2013), whereas removal of GLPG1837 from the solution readily brings the current back to the control level (Fig. 5, A and B). Technically, this tight binding of VX-770 makes it virtually impossible to obtain an accurate dose–response relationship to access its state-dependent binding. Looking into the physical properties of these two reagents, we noted a large difference in the partition coefficients (P) between VX-770 ($\log P = 6.34 \pm 0.78$) and GLPG1837 ($\log P = 3.22 \pm 0.73$). The hydrophobic nature of VX-770 explains why visible precipitates were seen at $[\text{VX-770}] > 1$ μM in our perfusion solution. We also speculate that this hydrophobicity property may partly account for the high affinities of VX-770. Although more studies are required to examine how VX-770 possesses a higher affinity yet lower efficacy than GLPG1837, our results support the aforementioned thermodynamic argument that efficacy and potency are two separate physicochemical properties of a ligand.

Regardless of the detailed mechanism, the state-dependent binding of potentiators demonstrated in the current work lays the foundation for guiding future designs of therapeutic strategies. The observation that

the apparent affinity of GLPG1837 is increased on dPATP-potentiated channels (and vice versa) raises the possibility of manipulating the effective concentration of one potentiator by first exposing the channels to another class of potentiators. In other words, combining two potentiators with different mechanisms of action not only results in pharmacological synergism in efficacy, but also mutually enhances their potency, which may be beneficial in a sense that such combination could lower the drug dosage used in clinics. In this aspect, experiments testing the idea of state-dependent binding for other CFTR potentiators are urgently needed. Moreover, we believe that a fundamental understanding of the mechanisms of action for CFTR potentiators, together with the exquisite molecular insights from the atomic structure of human CFTR (Liu et al., 2017), should pave the way for structure-based drug design targeting CFTR.

ACKNOWLEDGMENTS

We thank Cindy Chu and Shenghui Hu for their technical assistance and Drs. Ashvani Singh and Chris Tse for their helpful discussion. We also thank Galapagos/AbbVie for providing GLPG1837.

This work is supported by the National Institutes of Health (grant R01DK55835) and the Cystic Fibrosis Foundation (grant Hwang11P0) to T.-C. Hwang.

Part of the work is supported by a service agreement with AbbVie Inc. The authors declare no additional competing financial interests.

Author contributions: conception and design of experiments: H.-I. Yeh and T.-C. Hwang; collection and data analysis: H.-I. Yeh; interpretation of data: H.-I. Yeh and T.-C. Hwang; design of computer simulation program: Y. Sohma; drafting the article: H.-I. Yeh, Y. Sohma, K. Conrath, and T.-C. Hwang; it is confirmed that all authors approved the final version of the manuscript. All experiments were performed in Dalton Cardiovascular Research Center, University of Missouri-Columbia.

Richard W. Aldrich served as editor.

Submitted: 25 August 2017

Accepted: 10 October 2017

REFERENCES

- Aleksandrov, A.A., L. Aleksandrov, and J.R. Riordan. 2002. Nucleoside triphosphate pentose ring impact on CFTR gating and hydrolysis. *FEBS Lett.* 518:183–188. [https://doi.org/10.1016/S0014-5793\(02\)02698-4](https://doi.org/10.1016/S0014-5793(02)02698-4)
- Barry, P.J., N. Ronan, and B.J. Plant. 2015. Cystic fibrosis transmembrane conductance regulator modulators: The end of the beginning. *Semin. Respir. Crit. Care Med.* 36:287–298. <https://doi.org/10.1055/s-0035-1546821>
- Bear, C.E., C.H. Li, N. Kartner, R.J. Bridges, T.J. Jensen, M. Ramjessingh, and J.R. Riordan. 1992. Purification and functional reconstitution of the cystic fibrosis transmembrane conductance regulator (CFTR). *Cell.* 68:809–818. [https://doi.org/10.1016/0092-8674\(92\)90155-6](https://doi.org/10.1016/0092-8674(92)90155-6)
- Berg, J., J. Tymoczko, and L. Stryer. 2002. Chemical bonds in biochemistry. In *Biochemistry*. Fifth edition. WH Freeman, New York. Section 1.3.
- Bompadre, S.G., Y. Sohma, M. Li, and T.C. Hwang. 2007. G551D and G1349D, two CF-associated mutations in the signature sequences of CFTR, exhibit distinct gating defects. *J. Gen. Physiol.* 129:285–298. <https://doi.org/10.1085/jgp.200609667>

- Bompadre, S.G., M. Li, and T.C. Hwang. 2008. Mechanism of G551D-CFTR (cystic fibrosis transmembrane conductance regulator) potentiation by a high affinity ATP analog. *J. Biol. Chem.* 283:5364–5369. <https://doi.org/10.1074/jbc.M709417200>
- Cai, Z., A. Taddei, and D.N. Sheppard. 2006. Differential sensitivity of the cystic fibrosis (CF)-associated mutants G551D and G1349D to potentiators of the cystic fibrosis transmembrane conductance regulator (CFTR) Cl⁻ channel. *J. Biol. Chem.* 281:1970–1977. <https://doi.org/10.1074/jbc.M510576200>
- Chaves, L.A.P., and D.C. Gadsby. 2015. Cysteine accessibility probes timing and extent of NBD separation along the dimer interface in gating CFTR channels. *J. Gen. Physiol.* 145:261–283. <https://doi.org/10.1085/jgp.201411347>
- Cholon, D.M., N.L. Quinney, M.L. Fulcher, C.R. Esther Jr., J. Das, N.V. Dokholyan, S.H. Randell, R.C. Boucher, and M. Gentsch. 2014. Potentiator ivacaftor abrogates pharmacological correction of ΔF508 CFTR in cystic fibrosis. *Sci. Transl. Med.* 6:246ra96. <https://doi.org/10.1126/scitranslmed.3008680>
- Csanády, L. 2000. Rapid kinetic analysis of multichannel records by a simultaneous fit to all dwell-time histograms. *Biophys. J.* 78:785–799. [https://doi.org/10.1016/S0006-3495\(00\)76636-7](https://doi.org/10.1016/S0006-3495(00)76636-7)
- Csanády, L., and B. Töröcsik. 2014. Structure-activity analysis of a CFTR channel potentiator: Distinct molecular parts underlie dual gating effects. *J. Gen. Physiol.* 144:321–336. <https://doi.org/10.1085/jgp.201411246>
- Csanády, L., P. Vergani, and D.C. Gadsby. 2010. Strict coupling between CFTR's catalytic cycle and gating of its Cl⁻ ion pore revealed by distributions of open channel burst durations. *Proc. Natl. Acad. Sci. USA.* 107:1241–1246. <https://doi.org/10.1073/pnas.0911061107>
- Cui, L., L. Aleksandrov, Y.-X. Hou, M. Gentsch, J.-H. Chen, J.R. Riordan, and A.A. Aleksandrov. 2006. The role of cystic fibrosis transmembrane conductance regulator phenylalanine 508 side chain in ion channel gating. *J. Physiol.* 572:347–358. <https://doi.org/10.1113/jphysiol.2005.099457>
- Cui, L., L. Aleksandrov, X.B. Chang, Y.X. Hou, L. He, T. Hegedus, M. Gentsch, A. Aleksandrov, W.E. Balch, and J.R. Riordan. 2007. Domain interdependence in the biosynthetic assembly of CFTR. *J. Mol. Biol.* 365:981–994. <https://doi.org/10.1016/j.jmb.2006.10.086>
- Dalemans, W., P. Barbry, G. Champigny, S. Jallat, K. Dott, D. Dreyer, R.G. Crystal, A. Pavirani, J.P. Lecocq, and M. Lazdunski. 1991. Altered chloride ion channel kinetics associated with the delta F508 cystic fibrosis mutation. *Nature.* 354:526–528. <https://doi.org/10.1038/354526a0>
- Du, K., and G.L. Lukacs. 2009. Cooperative assembly and misfolding of CFTR domains in vivo. *Mol. Biol. Cell.* 20:1903–1915. <https://doi.org/10.1091/mbc.E08-09-0950>
- Du, K., M. Sharma, and G.L. Lukacs. 2005. The DeltaF508 cystic fibrosis mutation impairs domain-domain interactions and arrests post-translational folding of CFTR. *Nat. Struct. Mol. Biol.* 12:17–25. <https://doi.org/10.1038/nsmb882>
- Eckford, P.D., C. Li, M. Ramjeesingh, and C.E. Bear. 2012. Cystic fibrosis transmembrane conductance regulator (CFTR) potentiator VX-770 (ivacaftor) opens the defective channel gate of mutant CFTR in a phosphorylation-dependent but ATP-independent manner. *J. Biol. Chem.* 287:36639–36649. <https://doi.org/10.1074/jbc.M112.393637>
- Goodman, L.S. 2011. Goodman and Gilman's The Pharmacological Basis of Therapeutics. 12th edition. McGraw-Hill, New York. 77 pp.
- Gunderson, K.L., and R.R. Kopito. 1994. Effects of pyrophosphate and nucleotide analogs suggest a role for ATP hydrolysis in cystic fibrosis transmembrane regulator channel gating. *J. Biol. Chem.* 269:19349–19353.
- Gunderson, K.L., and R.R. Kopito. 1995. Conformational states of CFTR associated with channel gating: The role of ATP binding and hydrolysis. *Cell.* 82:231–239. [https://doi.org/10.1016/0092-8674\(95\)90310-0](https://doi.org/10.1016/0092-8674(95)90310-0)
- Hadida, S., F. Van Goor, J. Zhou, V. Arumugam, J. McCartney, A. Hazlewood, C. Decker, P. Negulescu, and P.D.J. Grootenhuus. 2014. Discovery of N-(2,4-di-tert-butyl-5-hydroxyphenyl)-4-oxo-1,4-dihydroquinoline-3-carboxamide (VX-770, ivacaftor), a potent and orally bioavailable CFTR potentiator. *J. Med. Chem.* 57:9776–9795. <https://doi.org/10.1021/jm5012808>
- Hwang, T.C., and D.N. Sheppard. 1999. Molecular pharmacology of the CFTR Cl⁻ channel. *Trends Pharmacol. Sci.* 20:448–453. [https://doi.org/10.1016/S0165-6147\(99\)01386-3](https://doi.org/10.1016/S0165-6147(99)01386-3)
- Hwang, T.C., and D.N. Sheppard. 2009. Gating of the CFTR Cl⁻ channel by ATP-driven nucleotide-binding domain dimerisation. *J. Physiol.* 587:2151–2161. <https://doi.org/10.1113/jphysiol.2009.171595>
- Hwang, T.C., F. Wang, I.C. Yang, and W.W. Reenstra. 1997. Genistein potentiates wild-type and delta F508-CFTR channel activity. *Am. J. Physiol.* 273:C988–C998.
- Jih, K.Y., and T.C. Hwang. 2013. Vx-770 potentiates CFTR function by promoting decoupling between the gating cycle and ATP hydrolysis cycle. *Proc. Natl. Acad. Sci. USA.* 110:4404–4409. <https://doi.org/10.1073/pnas.1215982110>
- Jih, K.Y., Y. Sohma, and T.C. Hwang. 2012. Nonintegral stoichiometry in CFTR gating revealed by a pore-lining mutation. *J. Gen. Physiol.* 140:347–359. <https://doi.org/10.1085/jgp.201210834>
- Jih, K.Y., W.Y. Lin, Y. Sohma, and T.C. Hwang. 2017. CFTR potentiators: From bench to bedside. *Curr. Opin. Pharmacol.* In press. <https://doi.org/10.1016/j.coph.2017.09.015>
- Kopeikin, Z., Y. Sohma, M. Li, and T.C. Hwang. 2010. On the mechanism of CFTR inhibition by a thiazolidinone derivative. *J. Gen. Physiol.* 136:659–671. <https://doi.org/10.1085/jgp.201010518>
- Kopeikin, Z., Z. Yuksek, H.Y. Yang, and S.G. Bompadre. 2014. Combined effects of VX-770 and VX-809 on several functional abnormalities of F508del-CFTR channels. *J. Cyst. Fibros.* 13:508–514. <https://doi.org/10.1016/j.jcf.2014.04.003>
- Lin, W.Y., K.Y. Jih, and T.C. Hwang. 2014. A single amino acid substitution in CFTR converts ATP to an inhibitory ligand. *J. Gen. Physiol.* 144:311–320. <https://doi.org/10.1085/jgp.201411247>
- Lin, W.Y., Y. Sohma, and T.C. Hwang. 2016. Synergistic potentiation of cystic fibrosis transmembrane conductance regulator gating by two chemically distinct potentiators, ivacaftor (VX-770) and 5-nitro-2-(3-phenylpropylamino) benzoate. *Mol. Pharmacol.* 90:275–285. <https://doi.org/10.1124/mol.116.104570>
- Liu, F., Z. Zhang, L. Csanády, D.C. Gadsby, and J. Chen. 2017. Molecular structure of the human CFTR ion channel. *Cell.* 169:85–95.e8. <https://doi.org/10.1016/j.cell.2017.02.024>
- Ma, T., J.R. Thiagarajah, H. Yang, N.D. Sonawane, C. Folli, L.J. Galietta, and A.S. Verkman. 2002. Thiazolidinone CFTR inhibitor identified by high-throughput screening blocks cholera toxin-induced intestinal fluid secretion. *J. Clin. Invest.* 110:1651–1658. <https://doi.org/10.1172/JCI0216112>
- Miki, H., Z. Zhou, M. Li, T.C. Hwang, and S.G. Bompadre. 2010. Potentiation of disease-associated cystic fibrosis transmembrane conductance regulator mutants by hydrolyzable ATP analogs. *J. Biol. Chem.* 285:19967–19975. <https://doi.org/10.1074/jbc.M109.092684>
- Ostedgaard, L.S., O. Baldursson, and M.J. Welsh. 2001. Regulation of the cystic fibrosis transmembrane conductance regulator Cl⁻ channel by its R domain. *J. Biol. Chem.* 276:7689–7692. <https://doi.org/10.1074/jbc.R100001200>
- Pedemonte, N., N.D. Sonawane, A. Taddei, J. Hu, O. Zegarar-Moran, Y.F. Suen, L.I. Robins, C.W. Dicus, D. Willenbring, M.H.

- Nantz, et al. 2005. Phenylglycine and sulfonamide correctors of defective delta F508 and G551D cystic fibrosis transmembrane conductance regulator chloride-channel gating. *Mol. Pharmacol.* 67:1797–1807. <https://doi.org/10.1124/mol.105.010959>
- Quinton, P.M., and M.M. Reddy. 1991. Regulation of absorption in the human sweat duct. *Adv. Exp. Med. Biol.* 290:159–170.
- Riordan, J.R., J.M. Rommens, B. Kerem, N. Alon, R. Rozmahel, Z. Grzelczak, J. Zielenski, S. Lok, N. Plavsic, J.L. Chou, et al. 1989. Identification of the cystic fibrosis gene: Cloning and characterization of complementary DNA. *Science.* 245:1066–1073. <https://doi.org/10.1126/science.2475911>
- Rosser, M.F.N., D.E. Grove, L. Chen, and D.M. Cyr. 2008. Assembly and misassembly of cystic fibrosis transmembrane conductance regulator: Folding defects caused by deletion of F508 occur before and after the calnexin-dependent association of membrane spanning domain (MSD) 1 and MSD2. *Mol. Biol. Cell.* 19:4570–4579. <https://doi.org/10.1091/mbc.E08-04-0357>
- Rowe, S.M., and A.S. Verkman. 2013. Cystic fibrosis transmembrane regulator correctors and potentiators. *Cold Spring Harb. Perspect. Med.* 3:a009761. <https://doi.org/10.1101/cshperspect.a009761>
- Rowe, S.M., S. Miller, and E.J. Sorscher. 2005. Cystic fibrosis. *N. Engl. J. Med.* 352:1992–2001. <https://doi.org/10.1056/NEJMra043184>
- Sohma, Y., and T.C. Hwang. 2015. Cystic Fibrosis and the CFTR Anion Channel. In *Handbook of Ion Channels*. CRC Press, Boca Raton, FL, 627–648. <https://doi.org/10.1201/b18027-48>
- Stratford, F.L., M. Ramjeesingh, J.C. Cheung, L.J. Huan, and C.E. Bear. 2007. The Walker B motif of the second nucleotide-binding domain (NBD2) of CFTR plays a key role in ATPase activity by the NBD1-NBD2 heterodimer. *Biochem. J.* 401:581–586. <https://doi.org/10.1042/BJ20060968>
- Thibodeau, P.H., C.A. Brautigam, M. Machius, and P.J. Thomas. 2005. Side chain and backbone contributions of Phe508 to CFTR folding. *Nat. Struct. Mol. Biol.* 12:10–16. <https://doi.org/10.1038/nsmb881>
- Tsai, M.F., H. Shimizu, Y. Sohma, M. Li, and T.C. Hwang. 2009. State-dependent modulation of CFTR gating by pyrophosphate. *J. Gen. Physiol.* 133:405–419. <https://doi.org/10.1085/jgp.200810186>
- Tsai, M.F., M. Li, and T.C. Hwang. 2010. Stable ATP binding mediated by a partial NBD dimer of the CFTR chloride channel. *J. Gen. Physiol.* 135:399–414. <https://doi.org/10.1085/jgp.201010399>
- Van Goor, F., S. Hadida, P.D. Grootenhuis, B. Burton, D. Cao, T. Neuberger, A. Turnbull, A. Singh, J. Joubbran, A. Hazlewood, et al. 2009. Rescue of CF airway epithelial cell function in vitro by a CFTR potentiator, VX-770. *Proc. Natl. Acad. Sci. USA.* 106:18825–18830. <https://doi.org/10.1073/pnas.0904709106>
- Van Goor, F., S. Hadida, P.D. Grootenhuis, B. Burton, J.H. Stack, K.S. Straley, C.J. Decker, M. Miller, J. McCartney, E.R. Olson, et al. 2011. Correction of the F508del-CFTR protein processing defect in vitro by the investigational drug VX-809. *Proc. Natl. Acad. Sci. USA.* 108:18843–18848. <https://doi.org/10.1073/pnas.1105787108>
- Van Goor, F., H. Yu, B. Burton, and B.J. Hoffman. 2014. Effect of ivacaftor on CFTR forms with missense mutations associated with defects in protein processing or function. *J. Cyst. Fibros.* 13:29–36. <https://doi.org/10.1016/j.jcf.2013.06.008>
- Veit, G., R.G. Avramescu, D. Perdomo, P.-W. Phuan, M. Bagdany, P.M. Apaja, F. Borot, D. Szollosi, Y.-S. Wu, W.E. Finkbeiner, et al. 2014. Some gating potentiators, including VX-770, diminish Δ F508-CFTR functional expression. *Sci. Transl. Med.* 6:246ra297. <https://doi.org/10.1126/scitranslmed.3008889>
- Veit, G., R.G. Avramescu, A.N. Chiang, S.A. Houck, Z. Cai, K.W. Peters, J.S. Hong, H.B. Pollard, W.B. Guggino, W.E. Balch, et al. 2016. From CFTR biology toward combinatorial pharmacotherapy: Expanded classification of cystic fibrosis mutations. *Mol. Biol. Cell.* 27:424–433. <https://doi.org/10.1091/mbc.E14-04-0935>
- Vergani, P., A.C. Nairn, and D.C. Gadsby. 2003. On the mechanism of MgATP-dependent gating of CFTR Cl⁻ channels. *J. Gen. Physiol.* 121:17–36. <https://doi.org/10.1085/jgp.20028673>
- Vergani, P., S.W. Lockless, A.C. Nairn, and D.C. Gadsby. 2005. CFTR channel opening by ATP-driven tight dimerization of its nucleotide-binding domains. *Nature.* 433:876–880. <https://doi.org/10.1038/nature03313>
- Wang, W., G. Li, J.P. Clancy, and K.L. Kirk. 2005. Activating cystic fibrosis transmembrane conductance regulator channels with pore blocker analogs. *J. Biol. Chem.* 280:23622–23630. <https://doi.org/10.1074/jbc.M503118200>
- Welsh, M.J., and A.E. Smith. 1993. Molecular mechanisms of CFTR chloride channel dysfunction in cystic fibrosis. *Cell.* 73:1251–1254. [https://doi.org/10.1016/0092-8674\(93\)90353-R](https://doi.org/10.1016/0092-8674(93)90353-R)
- Yang, H., A.A. Shelat, R.K. Guy, V.S. Gopinath, T. Ma, K. Du, G.L. Lukacs, A. Taddei, C. Folli, N. Pedemonte, et al. 2003. Nanomolar affinity small molecule correctors of defective Delta F508-CFTR chloride channel gating. *J. Biol. Chem.* 278:35079–35085. <https://doi.org/10.1074/jbc.M303098200>
- Yeh, H.I., J.T. Yeh, and T.C. Hwang. 2015. Modulation of CFTR gating by permeant ions. *J. Gen. Physiol.* 145:47–60. <https://doi.org/10.1085/jgp.201411272>
- Yu, H., B. Burton, C.J. Huang, J. Worley, D. Cao, J.P. Johnson Jr., A. Urrutia, J. Joubbran, S. Seepersaud, K. Sussky, et al. 2012. Ivacaftor potentiation of multiple CFTR channels with gating mutations. *J. Cyst. Fibros.* 11:237–245. <https://doi.org/10.1016/j.jcf.2011.12.005>
- Zhou, Z., X. Wang, M. Li, Y. Sohma, X. Zou, and T.C. Hwang. 2005. High affinity ATP/ADP analogues as new tools for studying CFTR gating. *J. Physiol.* 569:447–457. <https://doi.org/10.1113/jphysiol.2005.095083>
- Zielenski, J., and L.C. Tsui. 1995. Cystic fibrosis: Genotypic and phenotypic variations. *Annu. Rev. Genet.* 29:777–807. <https://doi.org/10.1146/annurev.ge.29.120195.004021>